MADRID
inter.noise 2019
June 16 - 19
NOISE CONTROL FOR A BETTER ENVIRONMENT

Aeroacoustic investigation of multirotor unmanned aircraft system (UAS) propellers and the effect of support structure

Kloet, Nicola[1] and Watkins, Simon [2] and Wang, Xu
RMIT University
Melbourne, Australia

ABSTRACT

The use of unmanned aircraft systems (UAS) or drones is growing, particularly for applications which must be performed near people, such as real-estate aerial photography. Urban UAS operations have led to noise is becoming an increasing concern for the community. The noise generated by a single typical multirotor UAS arm; including propeller and support structure, is investigated. Part of the measured noise arises from the propeller flow field and its interaction with the airframe support structure (arm). We have experimentally determined the acoustic emissions and wake of a typical UAS propeller in isolation, including 3-component velocity measurements at frequencies up to 2000 Hz. We also investigated the effect of the (highly 3D) flow field as it impinges on a typical airframe support structure. The results give guidelines for minimising this component of the aeroacoustically generated noise and recommendations are made for additional noise reduction.

Keywords: Unmanned Aircraft Systems (UAS), noise, aeroacoustic, flow-structure interactions, multirotor
I-INCE Classification of Subject Number: 13

1. UAS USE IN URBAN ENVIRONMENTS

Unmanned Aircraft Systems (UAS), or "drones", are employed for all kinds of payload delivery, information gathering, or entertainment purposes. Whether this is delivering pizza, taking photos for real estate advertisements or just for joy flights, these types of operations are increasingly conducted in urban environments.

UAS operations occurring near people pose a range of challenges, including safety, privacy, risk, performance, and societal acceptance. There has been a practical focus on the proper and safe integration of UAS into existing airspace in a way that can benefit all forms of aviation ((FAA), 2013) ((ESRG), 2013). Regulatory organisations have aready taken many of these issues into account.

One aspect that is difficult to address objectively is that of societal acceptance of this technology, and noise or acoustic emissions of UAS will be one key factor in garnering this acceptance. The uptake of UAS technology for missions such as package delivery requires infrastructure such as central depots. Residences close to such depots will be exposed to an increase in noise pollution, as will the delivery recipients and residents who are under flight paths. A change in noise exposure of 5-6dB can turn "sporadic complaints" into "widespread" (Environmental Protection Agency, 1971). Aside from the objective nature of an increase in noise exposure when discussing societal acceptance of

[1] nicola.kloet@rmit.edu.au
[2] simon.watkins@rmit.edu.au

UAS use is the fact that the perception of sound as a positive or negative thing depends heavily on the listener's attitude towards the sound source (Job, 1988). This psychoacoustic effect cannot be ignored when discussing UAS noise.

Manned aviation operations have long been commonplace, so many of the issues needing to be addressed for UAS can take inspiration from this area for solutions. Noise control with respect to manned aviation is relatively well documented, and there is a wealth of research regarding passenger comfort (Pennig, et al., 2012) and reducing noise exposure around airports (ICAO, 2016).

The focus of this work is multirotor UAS (MUAS) which have more in common with helicopters rather than fixed-wing aircraft. Noise reduction for helicopters has included efforts concerning propeller noise, engine, and gearbox noise (Magliozzi, et al., 1975). The focus on propeller noise extends to Blade Vortex Interaction (BVI) noise (JanakiRam, et al., 2009), thickness noise (Gopalan & Schmitz, 2010), and other methods of active noise cancelling (Shenggang, et al., 2014). Despite this research, the operating conditions and scale of these craft often mean the solutions cannot be applied directly to small consumer-style MUAS.

Recently, more attention has been given to the problem of MUAS noise as a whole (Intaratep, et al., 2016) (Kloet, et al., 2017) (Feight, et al., 2017) (Zawodny, et al., 2016), and even more specifically to the individual noise sources. One such source is the propulsion system, specifically the small UAS propellers (Boyer, et al., n.d.) (Leslie, et al., 2010) (Leslie, 2011) (Sinibaldi & Marino, 2013) (Serré, et al., n.d.). One feature of MUAS propeller noise that has not yet been addressed is that of the fluid-structure interaction between the propeller wake and the supporting structure. The physical architecture of many MUAS means a propeller blade passes over a supporting arm periodically which generates tonal noise at frequencies relevant to the blade passing frequency (BPF).

This paper describes an aeroacoustic investigation into commercially available propellers suitable for a MUAS of a similar scale to a DJI Phantom (9-inch diameter propellers). Propeller performance characteristics and wake flow fields are used to attempt to explain the acoustic profile generated in the presence of a supporting structure. The analysis is conducted in the context of annoyance in urban operations and noise mitigation strategies are suggested.

2. EXPERIMENTAL PROCEDURE

2.1 Equipment

Commercially available multirotor propellers were selected for testing from a range of manufacturers; the details of which are provided in Table 1. The drive system chosen was a KDE2315-850kV brushless motor and KDE 55-amp ESC running at 16.4 volts.

Table 1 - Propellers chosen for acoustic and performance testing

	Diameter (in.)	**Pitch (in.)**	**Manufacturer**	**Model**
A	9.0	3.0	Graupner	E-prop
C	9.0	4.3	HQ Prop	'DJI Phantom'
D	9.0	4.5	APC	MRP
E	9.0	4.5	HQ Prop	MRP
F	9.0	4.7	APC	Slow Fly
J	9.5	4.5	Tiger Motor	'DJI Phantom'

In order to gather performance data while taking acoustic measurements, an RC Benchmark Series 1580 Thrust Test Stand Dynamometer (shown in Figure 1), powered by an adjustable DC power supply, was used. This test stand and associated software was also able to measure and record relevant performance parameters such as thrust, Pulse Width Modulation (PWM) signal, Revolutions Per Minute (RPM), torque and temperature.

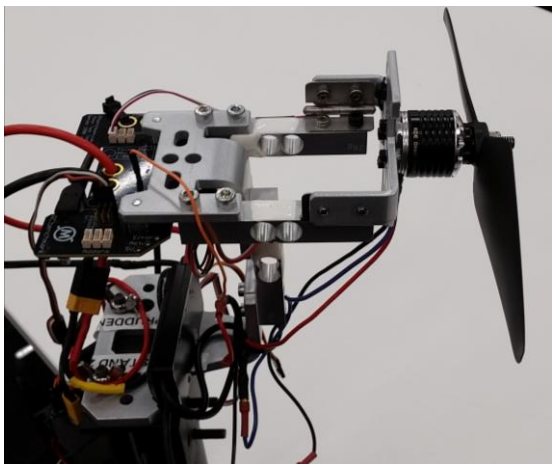

Figure 1 - RC Benchmark Series 1580 with selected propulsion system mounted (KDE2315-980kV motor and 55Amp ESC)

For acoustic measurements, a Brüel and Kjær Type 2235 Sound Pressure Level (SPL) meter fitted with a ½ inch condenser microphone was used. A National Instruments 6210 Data Acquisition unit made it was possible to capture both the overall SPL (OASPL), time and frequency data (frequency range 20 Hz to 20,000 Hz). Results were processed in a custom MATLAB script.

Turbulent Flow Instrumentation (TFI) Cobra Probes are multi-hole pressure probes able to capture the 3 orthogonal flow velocities (*u, v, w*) within a 90-degree cone of acceptance at a sample rate of 2000 Hz (Turbulent Flow Instrumentation Pty Ltd, 2018). A single probe was used for flow mapping the wake of the propellers after calibration in the RMIT Industrial Wind Tunnel.

2.2 Measurements

The SPL meter was mounted in a reflection-reducing box and placed 20 propeller radii away from the test stand, at an angle of 45 degrees to the thrust line (see Figure 2). Testing was conducted indoors, and calibrations revealed the ambient noise floor PSD <-90 Pa^2/Hz. All equipment was calibrated, and the measurement location was known to be in the far field.

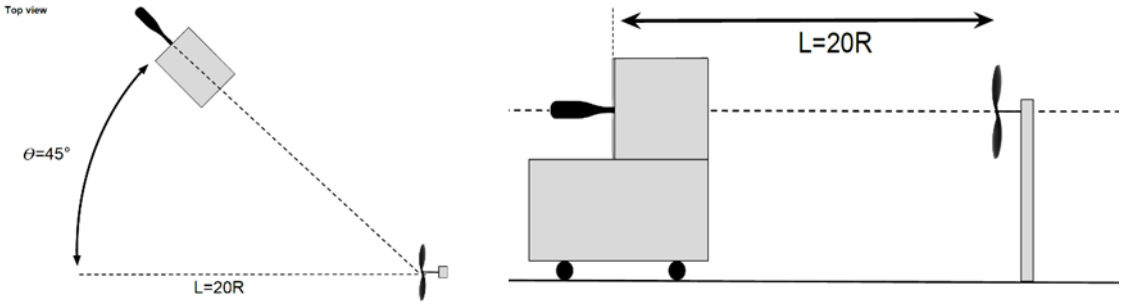

Figure 2 - Diagram of experimental layout. Top view (left) and side view (right)

For measurements where a supporting structure was introduced, two carbon fibre cylinders (diameter 25mm and 16mm, respectively) were placed in the propeller wake without being attached directly to the test stand. Circular cross sections were selected for two reasons: 1) they are quite common in multirotor architecture and 2) vortex shedding frequency can be calculated given the Strouhal number for cylinders is 0.2. The separation distance of 0.16R from the propeller plane indicates the distance that would be required if the propeller and motor were both directly mounted to the support structure (see Figure 3). Acoustic recordings were still made in the manner described above.

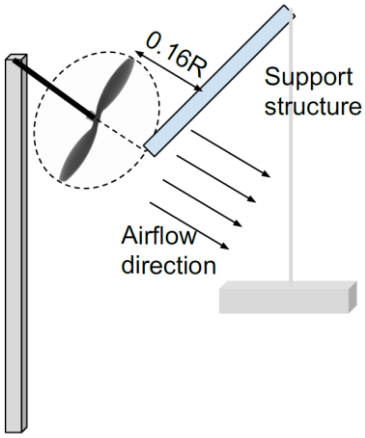

Figure 3 - Diagram of supporting structure influence testing

TFI Cobra Probe traversing system allowed measurements to be taken from the centre of the propeller disk, moving outwards along the radius in 1 cm increments, stopping after the propeller tip had been reached. Traverses were used to map the flow at several distances away from the propeller plane and a distance of 4 radii (4R) is presented here. Measurements include the three orthogonal velocities and flow angles within the probe's 90-degree cone of acceptance.

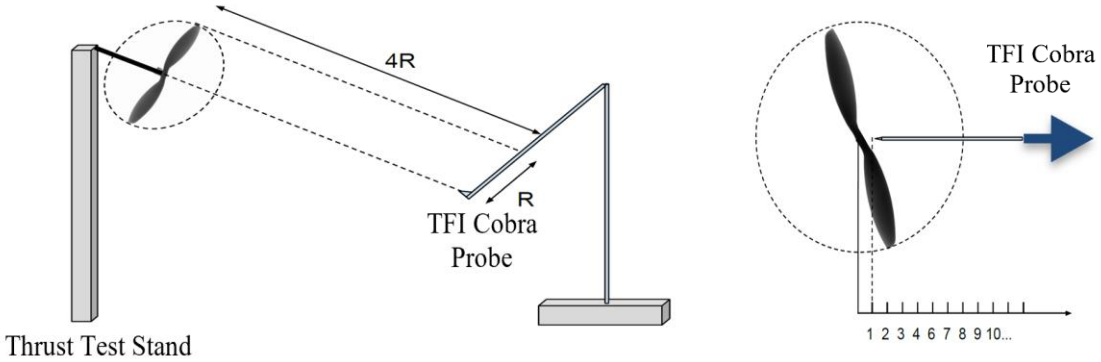

Figure 4 - TFI Cobra Probe traversing diagram. Overview (left) and radial traverse view (right)

3. RESULTS

3.1 Propeller Performance

The propellers were all tested for performance in terms of RPM and thrust generated. From this information it was possible to select appropriate test points in order to compare each of the propellers. Both thrust (500g, 800g, 1200g) and RPM (6000, 9000, 11000 RPM) points were selected.

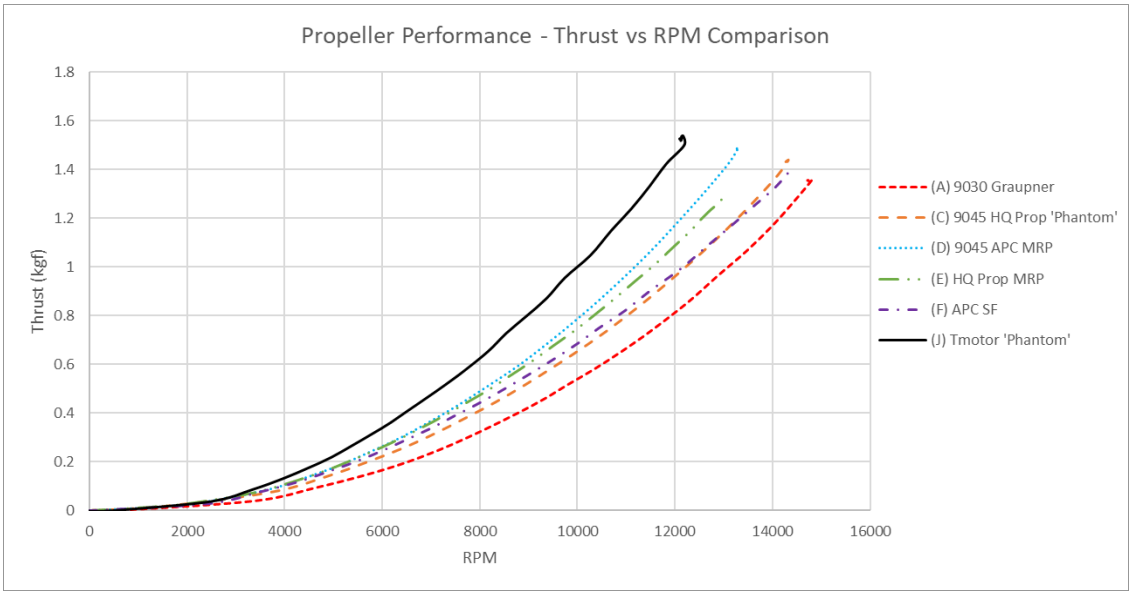

Figure 5 - Propeller performance comparison curves. Thrust (kg) versus rotational speed (RPM).

The maximum thrust differential between these propellers is 600g at 12,000RPM; see Figure 5. Likewise, to generate the same amount of thrust, 1.2kg for example, the RPM range is anywhere between 11,000 and 14,000 RPM depending on the propeller. This is explained by the individual geometry variations across propellers; larger blade areas, diameters and higher pitch angles will produce more thrust for a given RPM. This information is of use when designing an MUAS for a particular take-off weight and thus a specific propeller thrust requirement. For example, if designing with a propeller thrust requirement of 1.2kg, then the propeller capable of achieving that at lowest RPM seems likely to produce the lowest overall sound pressure level (OASPL). This is described in more detail in the next section.

3.2 Acoustics

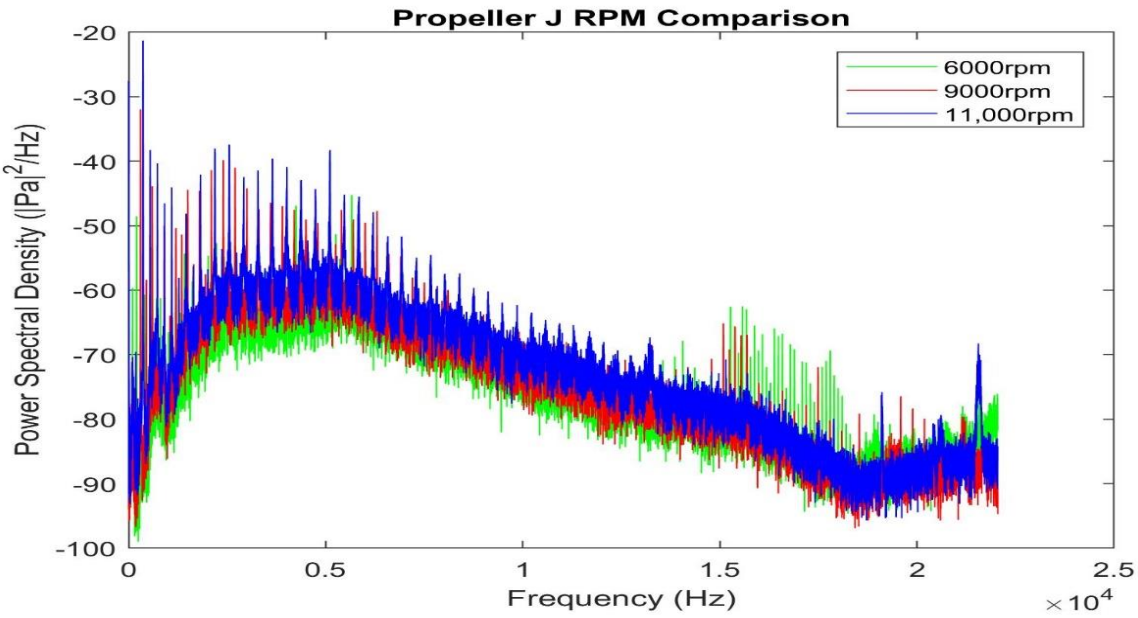

Figure 6 - Propeller J comparison of spectra at 3 RPM test points

Figure 6 demonstrates a comparison of propeller J at three different rotational speeds. Features of note for this plot (which were similar across the thrust comparison test points as well) include; 1) as RPM or thrust level increases, so does the OASPL. This makes choosing the propeller capable of providing sufficient thrust at the slowest RPM desirable from a low-noise perspective; 2) there are distinct tonal peaks which shift upwards in frequency corresponding to BPF and subsequent decaying harmonics; 3) there is additional tonal component for frequencies $15{,}000 < f < 18{,}000$ Hz present in lower RPM or thrust runs (green series). It is hypothesised that this caused by the motor noise which and it is masked by aerodynamically generated noise at higher rotational speeds.

When it comes to comparing the acoustic profile of different propellers, a spectral plot comparing propeller J (blue) and E (red) can be seen in Figure 7. These two propellers were chosen due to their apparent geometric similarities. The only differences discernible, based on the manufacturers' specifications, is that propeller J is 0.5 inches greater in diameter. This is for the test point of 11,000 RPM (note the blue series in Figure 6 is the same blue series shown in Figure 7). The tonal peaks present in the two acoustic profiles align with the expected BPF and decaying harmonics. However, the proportion of tonal noise present in the signal is much greater for propeller J than for propeller E. This was audible during recordings; propeller J had a noticeable musical-type "hum" whereas propeller E was comprised of mostly broadband "hissing" in comparison.

As for the mechanisms causing this difference in sound signature, one possibility is that propeller E may be experiencing some stall towards the root of the blades. The geometry is such that twisted propeller leads to high angle of attack in this region (a feature regarding which there is no manufacturer-provided information currently available). These two propellers do have different thrust levels at this test point (approximately 200 grams difference), some of which can be attributed to the larger diameter of propeller J and this is likely to have some effect on the overall sound profile. There may also be noise attributed to structural resonance which forms part of future work.

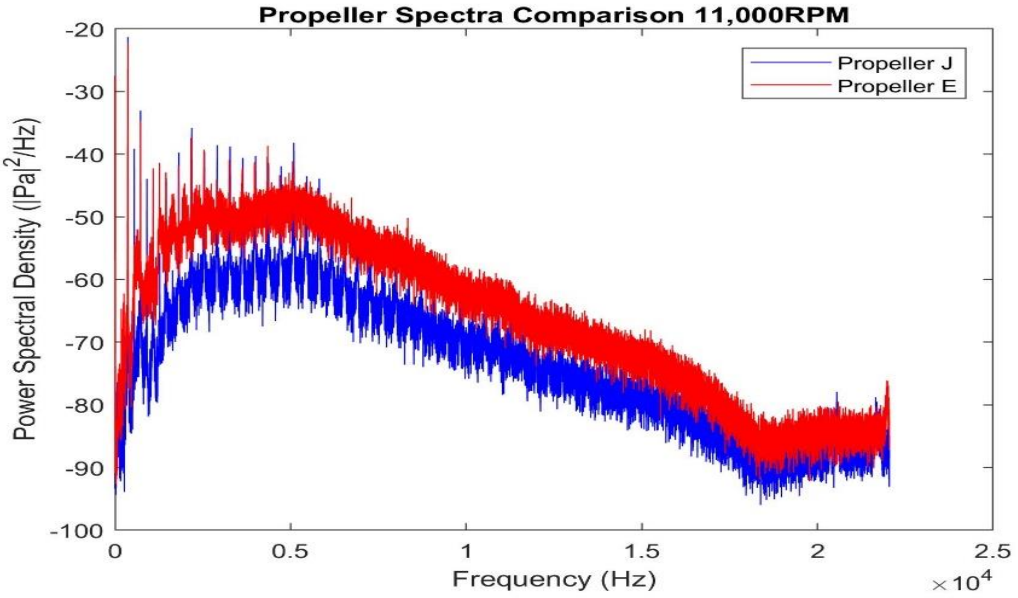

Figure 7 - Comparison of propellers J and E at 11,000 RPM test point

For a MUAS the wake flows over some kind of support structure. Figure 8 shows acoustic profiles for propeller J with no supporting structure in the wake (blue), with a 25mm diameter cylinder in the wake (red), and a 16mm diameter cylinder (green). This

example is for a moderate 9000 RPM and shows the three plots individually, as well as superimposed over one another (across the entire audible spectrum as well as in more detail at lower frequency ranges).

Anecdotal evidence indicated that changing the supporting structure would have a significant impact on the acoustic profile. These results indicate the effect, especially concerning tonal noise, is not as great as previously believed. There is a small increase in some tonal frequencies <~2000 Hz when a supporting structure is introduced into the wake of the flow. Variance in the amplitude of these tonal peaks could be attributed, in part, to inconsistencies between runs (see repeatability example in Figure 9 where tonal peaks had variances in amplitude of several dB at times). The gap between the propeller and the circular support structure was designed to mimic the distance of the motor used in this test, however there is a wide range of available brushless motor dimensions. It is possible that the acoustic signature is particularly sensitive to this distance, or that structural vibrations have a significant impact.

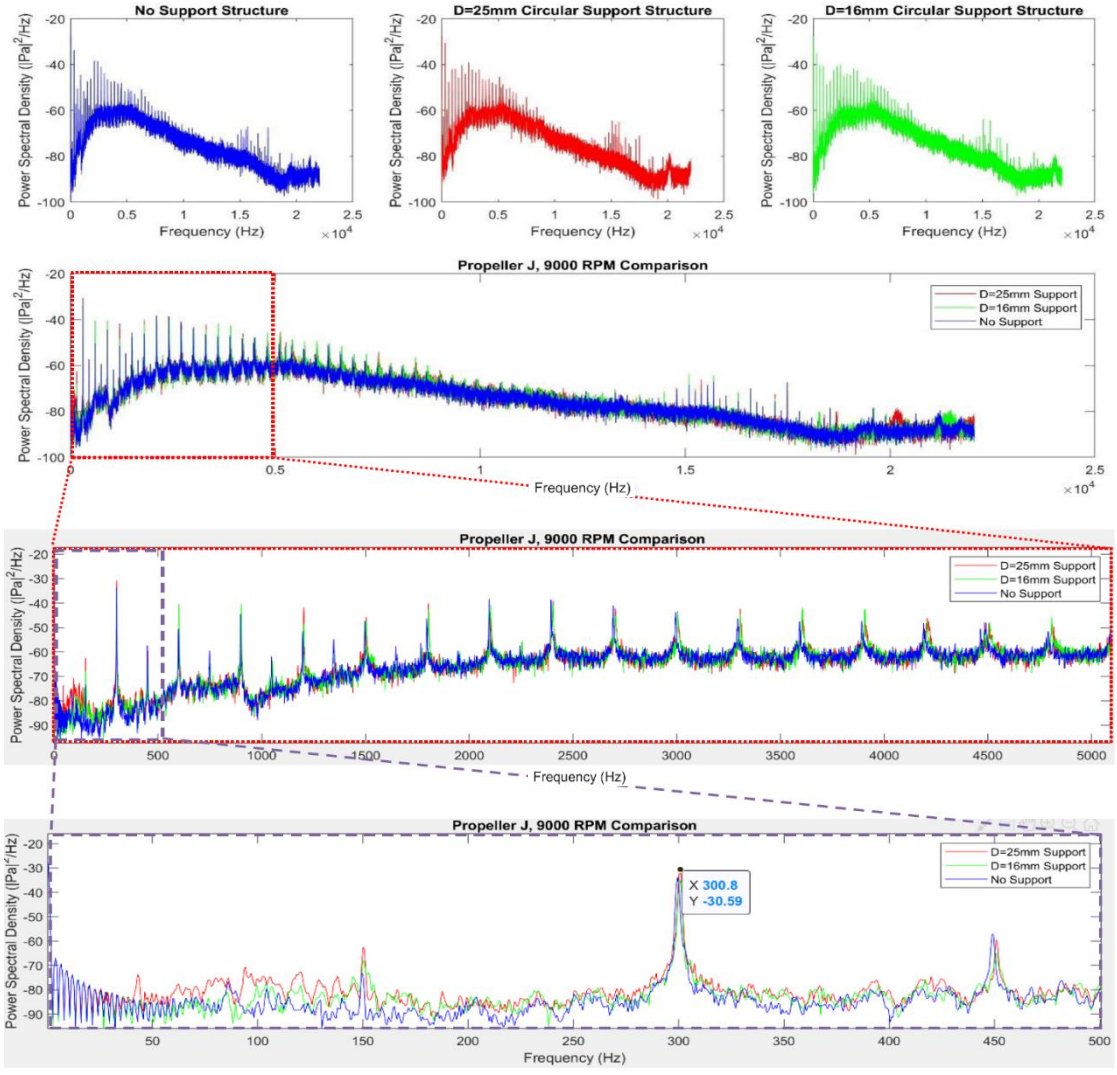

Figure 8 - Comparison of propeller J spectra with and without support structure in wake. Test condition: 9000RPM. Top (L to R): Spectrum without supporting structure (blue), spectrum with supporting structure 25mm diameter in wake (red), spectrum for propeller J with 16mm diameter supporting structure in wake (green).
Row 2: Comparison of all three conditions in top row.
Row 3: Detailed view of frequencies 0 to 5,000 Hz.
Row 4: Detailed view of frequencies 0 to 500 Hz.

The peak at 300 Hz exists at this RPM regardless of the fluid-structure interactions present, and subsequent harmonics are also accurately represented in all three conditions. It does seem that there is a marginal increase in power spectral density (PSD) when supporting structures of increasing diameter are introduced into the wake. This is most obvious in the bottom plot of Figure 8 at frequencies below 300 Hz.

Investigations into the repeatability of trials (Figure 9) have indicated that overall fidelity is good, however given the nature of the small differences between configurations in Figure 8 an improved calibration or more test runs may be required to converge upon a more accurate result. Some of the amplitudes in Figure 9 indicate small disparities between trials, most evident at the tonal peaks. A portion of this error could result from the ability of the test rig to hold a constant RPM, or perhaps a result of processing window lengths in the spectral calculations.

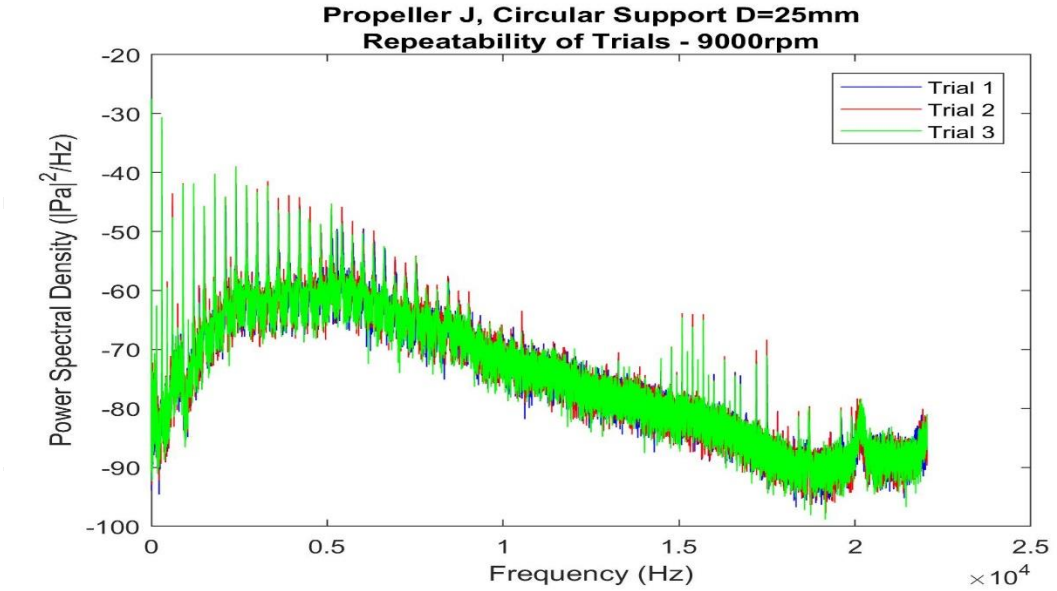

Figure 10 - Repeatability of trials under same test conditions: propeller J at 9000RPM with 25mm diameter support structure in wake

3.3 Aerodynamics

Figure 10 shows the average flow velocity magnitude of propeller wake at 4-radii from propeller plane (no supporting structure present). All the propellers tested indicate a similar profile, and the higher velocities correlate well with higher thrust levels in performance testing. Each series shown here is the average of three separate trials. These data had good repeatability across trials (<5%).

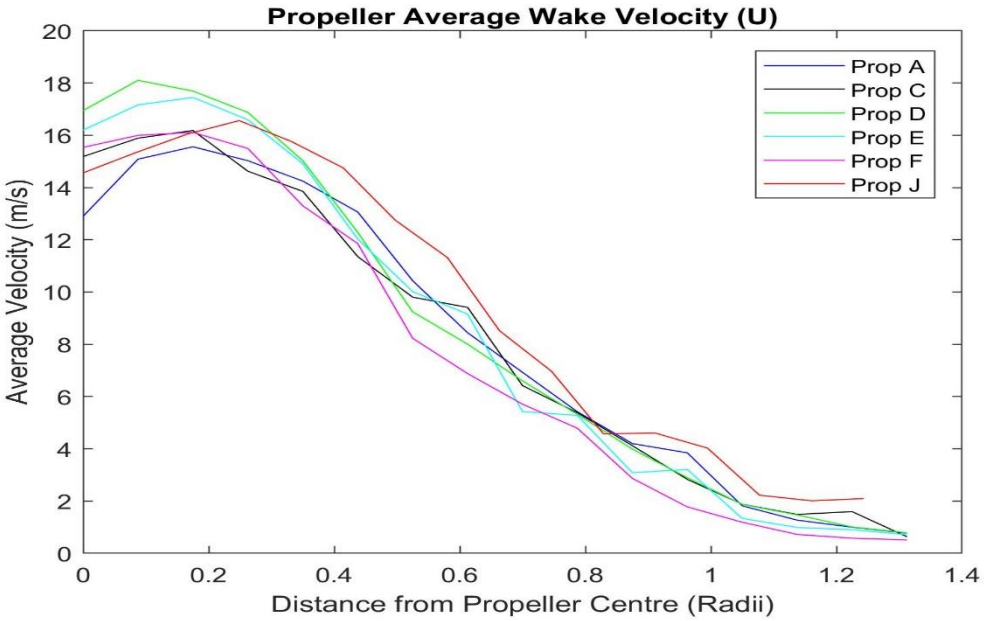

Figure 11 - Average wake velocity of propellers as measured 4 radii from propeller plane.

4. DISCUSSION

Given the Strouhal number for a circular cylinder, and the flow velocity are known from Cobra Probe measurements, it is possible to calculate the vortex shedding frequency of the flow around the supporting structure. The vortex shedding frequency varies, however, along the supporting structure due to the changing wake velocity of the propeller along the radius. It is possible that this effect, by default, contributes to changes in tonal noise. The rotating propeller also imparts swirl into the wake and this change in angularity of the flow and its effect on noise is something that is being investigated further.

Acoustic mitigation of MUAS noise is likely to be a combination of small efforts across different aspects of noise generation. Psychoacoustic sound design principles should be considered such that an overall noise reduction and change to a "pleasant" sound is achieved. Given the nature of the noise studied here, the reduction focus should initially be on the tonal (blade passing) frequencies since that type of noise is what many people find "annoying" (it has both temporal and tone colour relevance) with a secondary focus on the OASPL (Fastl & Zwickers, 2007).

Manufacturers should work towards improving the amount of information available to customers regarding the geometry of propeller. In many cases only pitch, diameter, and a model name are available. Some manufacturers specify a material but traditional aerodynamic descriptors such as aerofoil section, sweep, twist, and tip shapes are not readily available. This detailed information would help compare propellers more accurately and provide more insight into the geometry impacts on noise emissions. In the meantime, 3D laser scanning can provide digital models of these propellers.

5. CONCLUSIONS AND FUTURE WORK

Experimental method for characterising the aerodynamic and acoustic performance of multirotor unmanned aircraft system (MUAS) propellers is presented. The performance values (thrust and RPM) correlate well with the 3-component velocity measurements taken of the wake. Propeller geometry seems to have a much larger effect on the overall acoustic profile than any supporting structure used.

Additional flow mapping to provide more detail on sections of a propeller which may be stalling is underway, as well as wake mapping at a range of distances closer to the propeller plane. A more detailed investigation into vortex shedding from the supporting structure is also planned, along with testing the sensitivity of the distance between supporting structure and propeller plane as it pertains to noise. Finally an examination with how these features contribute to the psychoacoustic parameter "annoyance" with an aim of minimising the features most responsible.

5. ACKNOWLEDGEMENTS

This research was undertaken as part of the RMIT Unmanned Aircraft Systems Research Team, within the Sir Lawrence Wackett Aerospace Research Centre, at RMIT University. This work was supported by the Federal Government of Australia and the Defence Science Institute, an initiative of the State Government of Victoria.

6. REFERENCES

(ESRG), E. R. S. G., 2013. *Roadmap for the integration of civil remotely-piloted aircraft systems into the European Aviation System - Annex 2.* s.l.:s.n.

(FAA), F. A. A., 2013. *Integration of Civil Unmanned Aircraft Systems (UAS) in the National Airspace System (NAS) Roadmap,* s.l.: s.n.

Boyer, F. et al., n.d. *Multidisciplinary optimization of a MAV propeller for noise reduction.* s.l.:s.n.

Environmental Protection Agency, 1971. *Community Noise NTID300.3,* Washington D.C.: United States Environmental Protection Agency.

Farassat, F. & Succi, G. P., 1980. *A review of propeller discrete frequency noise prediction technology with emphasis on two current methods for time domain calculations.* s.l.:Elsevier.

Fastl, H. & Beidenhauser, G., 2014. *Psychoacoustic experiments on some unwanted interior car sounds.* s.l.:s.n.

Fastl, H. & Zwickers, E., 2007. *Psychoacoustics; Facts and Figures.* Third ed. Munich: Springer.

Feight, J. A., Whyte, S., Jacob, J. D. & Gaeta, R. J., 2017. *Acoustic Characterization of a Multi-Rotor UAS as a First Step Towards Noise Reduction.* s.l.:s.n.

Gelderblom, F. B., Gjestland, T. T., Granoien, I. L. & Taraldsen, G., 2014. *The impact of civil versus military aircraft noise on noise annoyance.* s.l.:s.n.

Gopalan, G. & Schmitz, F. H., 2010. *Helicopter thickness noise reduction possibilities through active on-blade acoustic control.* s.l.:s.n.

ICAO, ., 2016. *ICAO Environmental Report,* s.l.: s.n.

Intaratep, N. et al., 2016. *Experimental study of quadcopter acoustics and performance at static thrust conditions.* s.l.:s.n.

JanakiRam, R. D., Sim, B. W., Kitaplioglu, C. & Straub, F. K., 2009. *Blade-Vortex Interaction Noise Characteristics of a Full-Scale Active Flap Rotor.* s.l.:s.n.

Job, R., 1988. Community response to noise: A review of factors influencing the relationship between noise exposure and reaction. *The Journal of the Acoustical Society of America,* 83(3), pp. 991--1001.

Kloet, N., Watkins, S. & Clothier, R., 2017. *Acoustic signature measurement of small multi-rotor unmanned aircraft systems.* s.l.:SAGE Publications Sage UK: London, England.

Kloet, N. et al., 2017. *Drone on: A preliminary investigation of the acoustic impact of unmanned aircraft systems (UAS).* s.l.:s.n.

Leslie, A., 2011. *Broadband Noise Reduction of a Small UAV Propeller.* s.l.:s.n.

Leslie, A., Wong, K. & Auld, D., 2010. *Experimental analysis of the radiated noise from a small propeller.* s.l.:s.n.

Leslie, A., Wong, K. C. & Auld, D., 2008. *Broadband noise reduction on a mini-UAV propeller.* s.l.:s.n.

Magliozzi, B., Metzger, F., Bausch, W. & King, R., 1975. *A comprehensive review of helicopter noise literature.* s.l.:s.n.

Organization, I. C. A., 2011. *Cir 328 AN/190 Unmanned Aircraft Systems (UAS).* s.l.:s.n.

Pennig, S., Quehl, J. & Rolny, V., 2012. Effects of aircraft cabin noise on passenger comfort.. *Ergonomics,* 55(10), pp. 1252--65.

Sadasivan, S., Gurubasavaraj, M. & Sekar, S. R., 2001. *Acoustic signature of an unmanned air vehicle exploitation for aircraft localisation and parameter estimation.* s.l.:Defence Scientific Information \& Documentation Centre.

Serré, R., Chapin, V., Moschetta, J. & Fournier, H., n.d. *Reducing the noise of Micro--Air Vehicles in hover.* s.l.:s.n.

Shenggang, Y., Dakai, T., Xiaonei, Z. & Haoxin, Y., 2014. *Design of active noise control system applied to helicopter cabins.* s.l.:s.n.

Sinibaldi, G. & Marino, L., 2013. *Experimental analysis on the noise of propellers for small UAV.* s.l.:Elsevier.

Turbulent Flow Instrumentation Pty Ltd, 2018. *Cobra Probes.* [Online]
Available at: https://www.turbulentflow.com.au/Products/CobraProbe/CobraProbe.php
[Accessed 15 February 2019].

Wild, G., Murray, J. & Baxter, G., 2016. *Exploring civil drone accidents and incidents to help prevent potential air disasters.* s.l.:Multidisciplinary Digital Publishing Institute.

Zawodny, N. S., Boyd Jr, D. D. & Burley, C. L., 2016. *Acoustic Characterization and Prediction of Representative, Small-Scale Rotary-Wing Unmanned Aircraft System Components.* s.l.:s.n.

Zawodny, N. S., Christian, A. & Cabell, R., 2018. *A Summary of NASA Research Exploring the Acoustics of Small Unmanned Aerial Systems.* s.l.:s.n.